



LAWRENCE
LIVERMORE
NATIONAL
LABORATORY

Fabrication and testing of diamond-machined gratings in ZnSe, GaP, and bismuth germanate for the near infrared and visible

P. J. Kuzmenko, S. L. Little , Y. Ikeda, N.
Kobayashi

June 27, 2008

SPIE Advanced Optical and Mechanical Technologies in
Telescopes and Instrumentation
Marseille, France
June 23, 2008 through June 28, 2008

Disclaimer

This document was prepared as an account of work sponsored by an agency of the United States government. Neither the United States government nor Lawrence Livermore National Security, LLC, nor any of their employees makes any warranty, expressed or implied, or assumes any legal liability or responsibility for the accuracy, completeness, or usefulness of any information, apparatus, product, or process disclosed, or represents that its use would not infringe privately owned rights. Reference herein to any specific commercial product, process, or service by trade name, trademark, manufacturer, or otherwise does not necessarily constitute or imply its endorsement, recommendation, or favoring by the United States government or Lawrence Livermore National Security, LLC. The views and opinions of authors expressed herein do not necessarily state or reflect those of the United States government or Lawrence Livermore National Security, LLC, and shall not be used for advertising or product endorsement purposes.

Fabrication and testing of diamond-machined gratings in ZnSe, GaP, and bismuth germanate for the near infrared and visible

Paul J. Kuzmenko^{a*}, Steve L. Little^a, Yuji Ikeda^b, and Naoto Kobayashi^c

^aLawrence Livermore National Laboratory, L-183 PO Box 808, Livermore, CA 94551;

^bPhotocoding Inc., 3-16-8-101 Higashi-Hashimoto, Sagamihara, Kanagawa 229-1104, Japan;

^cInstitute of Astronomy, University of Tokyo, 2-21-1, Osawa, Mitaka, Tokyo 181-0015, Japan

ABSTRACT

High quality immersion gratings for infrared applications have been demonstrated in silicon and germanium. To extend this technology to shorter wavelengths other materials must be investigated. We selected three materials, zinc selenide, gallium phosphide and bismuth germanate ($\text{Bi}_4\text{Ge}_3\text{O}_{12}$), based on high refractive index, good visible transmission and commercial availability in useful sizes. Crystal samples were diamond turned on an ultra-precision lathe to identify preferred cutting directions. Using this information we diamond-flycut test gratings over a range of feed rates to determine the optimal cutting conditions. For both ZnSe and GaP good surface quality was achieved at feed rates up to 1.0 cm/minute using a special compound angle diamond tool with negative rake angles on both cutting surfaces. The surface roughness of the groove facets was about 4 nm. A Zygo interferometer measured grating wavefront errors in reflection. For the ZnSe the RMS error was $< \lambda/20$ @633nm. More extensive testing was performed with a HeNe laser source and a cooled CCD camera. These measurements demonstrated high relative diffraction efficiency ($> 80\%$), low random groove error (2.0 nm rms), and Rowland ghost intensities at $< 0.1\%$. Preliminary tests on bismuth germanate show high tool wear.

Keywords: immersion grating, zinc selenide, gallium phosphide, bismuth germanate, diamond machining

1. INTRODUCTION

Immersion gratings have been reported in silicon¹ and germanium² that are of high optical quality and suitable for use in real instruments. With good transmission from 1.2 to approximately 6 μm for silicon and from 2 to approximately 14 μm for germanium, the major infrared windows in atmospheric transmission can be covered. One may ask if these technologies can be extended into the near infrared and visible regions. The history of immersion gratings shows that they were originally proposed for the visible region using optical glass as the immersion material³. But the relatively low refractive index limits the benefits of immersion relative to the higher index materials available in the infrared. Some limited work has been done in fabricating immersion gratings and grisms in high index materials other than silicon or germanium but the applications have always been for the infrared^{4,5,6}. Optical quality was not high enough for use in the visible spectrum.

With improvements in diamond machining technology a wide range of materials may be considered for grating substrates. A recent paper speculated on the potential of gallium arsenide, gallium phosphide, zinc sulfide and zinc selenide for high index machined gratings in the near infrared and visible⁷. These materials are available commercially in sizes large enough to be of interest, although the machinability of gallium phosphide had yet to be determined. Some work also remained on demonstrating good transmission, especially at the shorter wavelengths, in commercial grade material. Another family of commercially available crystals with good short wavelength transmission are the radiation scintillators⁸. Bismuth germanate ($\text{Bi}_4\text{Ge}_3\text{O}_{12}$) is a scintillator⁹ with a refractive index greater than 2 and is a potential substrate for a short wavelength immersion grating. This work will extend the previous paper by reporting machined gratings in several of the most promising materials.

Section 2 reviews the choice of materials. Section 3 gives an overview of the machining process. Section 4 reports fabrication and testing of a ZnSe immersion grating. Section 5 discusses fabrication and testing of a GaP grating.

*kuzmenko1@llnl.gov; phone 925-423-4346; fax 925-422-2499

Preliminary results for the machining of bismuth germanate are found in section 6. A summary and conclusions are presented in section 7.

2. MATERIAL SELECTION

Several factors entered into the choice of materials for the test gratings. Since we are trying to fabricate visible and near infrared gratings, the primary consideration is good transmission and high refractive index in those spectral regions. It is important that the material be crystalline as amorphous materials can suffer from compositional and therefore refractive inhomogeneities. One would prefer a single crystal as the crystal axes will then maintain the same orientation to the direction of cut throughout the machining process. If this is not possible, then the crystal grains should be small so that minimal damage results if a grain is pulled out of the substrate during the machining. Another requirement is that the material be optically isotropic. Any birefringence would cause the diffraction angles to vary with polarization. Of course the material must be commercially available in sizes that allow fabrication of useful components. It also must be diamond machinable, not so hard that it causes excessive tool wear.

A comprehensive table of the optical properties of crystals such as that found in the Handbook of Optics¹⁰ is a good place to start the search. One finds that the highest index materials are generally those containing elements of the highest atomic weight. Simple diatomic molecules are most likely to yield isotropic crystals. The best candidates turn out to be the semiconductors ZnSe and GaP, which are grown commercially. Both zinc selenide and gallium phosphide crystals have a yellow orange color, which indicates that they have good transmission down to about 600 nm. For shorter wavelength applications other high index materials must be found. The materials considered for immersion gratings have been mostly semiconductors due to the commercial infrastructure that has built up to produce high quality crystals for electronic and optoelectronic applications. However the growth of wider bandgap semiconductors, such as gallium nitride, is technologically difficult. It is much easier to grow an epitaxial layer than a full crystal and this is industry's current strategy. So we must look elsewhere.

Another class of materials grown in useful sizes are scintillation crystals for radiation detection. These must have good transmission down to the short wavelength edge of the visible spectrum where radiation-induced fluorescence occurs and contain heavy atoms for good absorption of charged particles and gamma rays. Common scintillators include barium fluoride, thallium doped sodium iodide, and cadmium tungstate. Bismuth germanate ($\text{Bi}_4\text{Ge}_3\text{O}_{12}$), also known as BGO, is another scintillation crystal used in radiation detection. It fluoresces in the blue when excited by hard x-rays or charged particles. It has good transmission down to about 350 nm. The absorption at 480 nm is about 0.001/cm. Compared to most crystals that are transparent in this region the refractive index is quite high, about 2.152 at 480 nm¹¹. BGO has a cubic structure, which means that it is optically isotropic and lacks natural birefringence. Bismuth germanate is the third candidate for visible spectrum immersion gratings.

3. MACHINING PROCESS

The process of diamond flycutting an immersion grating into a brittle material has been described in much detail in previous publications on germanium gratings^{2,12}. Here we will only discuss issues unique to short wavelength operation. It is obvious that tolerances will shrink as wavelengths decrease. This puts tighter limits on machine vibration both from internal and external sources. Greater attention must be paid to long term environmental stability of the machining area as the tolerance for dimensional drift will be less.

As the operating wavelength decreases into the visible region, the grating pitch must also decrease in order to maintain the same grating order. Immersion gratings for short wavelengths will therefore have relatively small pitch. In order to achieve high diffraction efficiency, the radius of the corner in which the groove facets intersect must be small compared to the grating pitch. Previous work with germanium showed that it was possible to obtain very small radii, of order 0.1 μm by using a dead sharp diamond tool. However, the cutting speed had to be greatly reduced to avoid severe chipping of the groove facets. This is a problem with small pitch grating for the visible. When the total length of grooves to be cut has increased with the groove density, and the cutting speed has greatly decreased, practical limits in fabrication time will soon be reached.

A standard cutting tool for germanium has a negative rake angle on a single cutting surface. This means that the tool face is tipped forward from the perpendicular to the cutting direction (see figure 1) at the point of contact with the workpiece. A negative rake angle applies a compressive force to the substrate allowing a ductile cut to be made. To machine a grating the two facets forming the groove must be cut simultaneously, requiring two cutting surfaces intersecting in a sharp point. The facet not cut by a negative rake surface tends to chip severely unless cut very slowly. Recent work with a compound angle tool (i.e. one with a negative rake angle on both cutting surfaces) has shown that it is possible to get high quality facets at more practical feed rates, approaching 1 inch per minute. See figure 2 for an illustration of the tool.

One of the lessons learned from germanium was that the maximum thickness of material that could be removed in a single cut varies with the orientation of the direction of cut with respect to the crystal axes. This is true even for a cubic crystal because the density of atoms varies in the different crystal planes. With new materials some experimentation is required to determine the optimal cutting directions and machining parameters.

4. FABRICATION AND TESTING OF A ZINC SELENIDE GRATING

We previously mentioned the benefits of machining single crystal material. However, ZnSe undergoes a phase transition from a hexagonal wurtzite structure to a cubic zincblende structure at 1425°C, which is 90 degrees below its melting point (solidification temperature). As a result it is nearly impossible to grow high quality crystals from a melt¹³. Single crystals of ZnSe have been grown by the chemical vapor transport process, which involves the chemical constituents reacting in vapor phase and depositing on a seed crystal. They are limited in size to about 25 mm. All optical grade zinc selenide that is commercially available is polycrystalline. Very large slabs can be grown by chemical vapor deposition (CVD), although their thickness is limited by the speed of the growth process (~100µm/hour). This is the only way to get large blanks of ZnSe.

We chose standard polycrystalline window blanks 1.0 inch in diameter and 0.25 inch thick, as substrates for our test gratings. The blanks were polished on one side and rough ground on the other side, the one to be machined. We purchased a compound angle diamond tool with 30° negative rake on both cutting surfaces. It was specified to cut 90° grooves with a 25° blaze angle. Since the grains in a polycrystalline material have random orientation there is no preferred cutting direction, so it only remains to optimize the cutting speed.

We carried out a study using the compound angle diamond tool in which the feed rate of the Precision Engineering Research Lathe (PERL II) was varied in increments of 0.1 inch/minute from 0.1 to 1.0 inch per minute. At each feed rate a 2 mm wide segment of 30 µm pitch grooves were cut across the ZnSe disc. The test ruling covered half of the disc area. This was done at a constant spindle speed of 1000 rpm. Odorless mineral spirits were used as a cutting fluid and coolant. After removing the sample from the machine, it was cleaned with solvent, dried and examined under an optical microscope. A very small amount of chipping of the groove tips can be seen at the lowest feed rates. The chipping increases rapidly with feed rate above 0.4 inch/minute.

We examined the grooves further with a Veeco optical profilometer. A 3D plot of a region cut at 0.3 inch/minute is shown in figure 3. Data from a fairly clean area indicates an average surface roughness of 4 nm and an rms roughness of 5 nm (see figure 4). In some other regions of the surface the profile of the nominally flat groove facets shows deviations above the baseline but few deviations below the baseline. This indicates that excess roughness may be due to particulates on the surface rather than any irregularities in the cutting process.

Scanning electron microscope (SEM) images taken of the ZnSe ruling can be seen in figure 5. Similar to earlier gratings in germanium the surfaces appear very smooth and the corners and edges of the groove facets appear very sharp. As the Veeco had indicated, there are some particulates remaining on the surface even after the normal cleaning process. ZnSe is an electrical insulator so cutting debris might be held in place by electrostatic attraction.

We measured the blaze angle using the technique described by Loewen and Popov¹⁴ in which the grating is set up on a rotary stage in Littrow mode. The stage is then rotated to locate the zero order of diffraction and the two brightest diffraction orders. The blaze angle is deduced by interpolating between the brightest orders weighted by the diffracted power in those orders. We measured the blaze of the steeper of the two facets (nominally 65°) to be 61.7° and the shallow facet (nominally 25°) to be 22.5°. The discrepancy likely reflects an error in the shaping of the diamond tool.

A critical test of grating quality is the amount of aberration in the diffracted wavefront. This is readily measured by examining the diffracted wave reflected from the grating using an interferometer. Measurements from the 30 μm pitch ZnSe grating made with a Zygo interferometer operating are shown in figure 6. Deviation from a plane wave (grooves perfectly flat and aligned with each other) at 633 nm is 0.30 wave peak to valley and 0.030 wave rms.

More comprehensive testing¹⁵ was performed with the setup shown in figure 7. Here the grating is illuminated with a collimated HeNe beam. Diffracted light is collected by the lens and focused onto a CCD array. One can then view the intensities of the diffracted orders and compare them to theoretical predictions. As seen in figure 8, the energy concentration to a target order is very high. We examined four orders ($m=81, 82, 83$, and 84) around the peak of the blaze. The relative energy distribution to each order is 3% for $m=81$, 32% for $m=82$, 64% for $m=83$, and $< 1\%$ for $m=84$. 95% of energy is concentrated into the central two orders $m=82$ and $m=83$. (Since 633 nm is not a perfect blaze wavelength, the diffracted light does not concentrate into a single order.) This means that the blaze shape is nearly ideal. The background continuum between orders is very low ($\sim 1.3\%$), which suggests that the random error of the groove pitch is 6.3nm (rms).

If one views the intensity of the diffracted orders on a logarithmic scale, one sees weak peaks between the orders. Most of these can be explained as the result of diffraction by a finite number (~ 50) of grooves in the beam. There is stronger peak (up to 5%) that can be seen exactly halfway between diffraction orders. However the intensity varies as one probes around the grating. It is zero in regions where there is no chipping and highest in regions with the most severe chipping. If the chipping works as a shadow, then it would double the grating pitch (from d to $2d$) around the chipping point. We could then observe the diffraction orders of a pseudograting with a period of $2d$ at the center of main orders. The amplitude of grating ghosts other than those described above is less than 0.1%, corresponding to a periodic error amplitude of less than 1.8 nm. So the machined grating appears to be relatively ghost free except in regions where the ZnSe facets show some chipping.

We later cut a 150 μm pitch grating on the unused half of the same blank. Particulate contamination was much worse owing to the much larger volume of material that had to be removed during the cutting process. A peel off coating was found to do an excellent job of removing the particulates¹⁶. Values of surface roughness and wavefront error were similar to the 30 μm pitch grating and chipping was still an issue.

5. FABRICATION AND TESTING OF A GALLIUM PHOSPHIDE GRATING

Since no previous reports of diamond machined gallium phosphide appear in the literature, our first step was to obtain a sample of material and attempt to machine it. Single crystal GaP is used as a substrate for LED's and wafers are commercially available. We purchased a single crystal wafer of undoped GaP (carrier density of $< 1e16$ per cm^3) 50.8 mm diameter and 300 μm thick. The surface was polished on one side, lapped and etched on the other. It was oriented in the (100) direction. Previous work on germanium has shown that single crystals have a preferred cutting direction in which the deepest cut can be made without fracture of the material. Cutting along a preferred direction allows the fastest feed rates and hence the shortest fabrication time.

The GaP wafer was mounted in a vacuum chuck on an ultraprecision lathe and turned on the etched surface with a single point diamond tool to observe the change in surface finish with the direction of cut. Figure 9 shows the results of this experiment. One can see the four-fold symmetry of the "bad" cutting directions. The reference flat seen on the right side the wafer is in the (110) direction, a good cutting direction. We cleaved a piece of the wafer roughly 8 mm x 20 mm along the (110) direction to cut a grating using the same tool that was used on the ZnSe. As before we used a range of feed rates in increments on 0.1 inch/minute from 0.1 to 1.0 inch per minute to determine the optimum cutting conditions. Profilometer measurements showed an increase in surface roughness at feed rates above 0.4 inch/minute at 1000 rpm spindle speed. The surfaces looked good with no evidence of chipping. There was none of the particulate debris seen in the ZnSe. An SEM photo of groove detail may be seen in figure 10. Figure 11 shows the results of profilometry on GaP grooves cut at 0.4 inch/minute. The average roughness is about 6 nm (see figure 12). No Zygo measurements were made to determine wavefront error as thin wafers are too flexible to be very flat and it would be impossible to distinguish machining error from wafer bending. In hindsight the measurements may have been possible with the wafer was still mounted in the cutting fixture.

6. PRELIMINARY RESULTS WITH BISMUTH GERMANATE (BGO)

BGO crystals are grown from a melt by a low thermal gradient Czochralski process¹⁷ and are available commercially in sizes of a few inches. Laboratories in Russia have the capability to grow very large crystals of BGO, up to 13 cm diameter and 40 cm long¹⁸. We purchased a small polished BGO crystal (10 mm x 10 mm x 0.5 mm) cut in the (100) plane for diamond machining experiments. For the first test we fastened the crystal to the spindle with a urethane adhesive (see figure 13) and attempted to machine the surface. At a spindle speed of 1000 RPM, a tool tip radius of 0.02 inches, a 0.5 μm depth of cut and a feed rate of 0.011 inch per minute, we achieved an average surface roughness of 7.7 nm. Unfortunately a high rate of wear in the diamond tool was observed that could limit the usefulness of this material. It is possible that this excess wear may be result of abrasive material embedded in the BGO during the polishing process. This matter will be studied further.

7. SUMMARY AND CONCLUSIONS

The results of this study indicate that it is possible to diamond machine immersion gratings into ZnSe and GaP for the near infrared and visible. The optimal machining conditions for these new materials were determined. ZnSe appears to have a tendency to chip at the groove tips, which has the unfortunate consequence of producing grating ghosts similar to those caused by periodic ruling errors. Work remains to determine whether this chipping is fundamental to zinc selenide or to the polycrystalline nature of our blanks. If the latter it may be possible to develop a machining protocol (e.g. rough cut followed by a very shallow finishing cut) to achieve acceptable results. Single crystal gallium phosphide was free from chipping but work needs to be done to verify the optical transmission at shorter wavelengths in commercial grade material. Finally BGO has very promising optical properties and is available in large sizes, but preliminary results indicate high wear in the diamond tool. This reduces the utility of this material.

8. ACKNOWLEDGEMENTS

I would like to acknowledge Jim Ferreira for taking the SEM photographs and to Marcia Kellam for measurements with the Zygo interferometer. Thanks are also due to Joe Galkowski for freeing up enough "free energy" to demonstrate the initial concepts and also to Dave Hopkins for putting in long hours after finishing up his "day job" to tune the control loops of the PERL lathe. This work was performed under the auspices of the U.S. Department of Energy by Lawrence Livermore National Laboratory in part under Contract W-7405-Eng-48 and in part under Contract DE-AC52-07NA27344.

9. REFERENCES

1. J.P. Marsh, D.J. Mar and D.T. Jaffe, "Production and evaluation of silicon immersion gratings for infrared astronomy," *Applied Optics* **46** pp. 3400-3416, 2007.
2. P. J. Kuzmenko, P. J. Davis, S. L. Little, L. M. Little and J. V. Bixler, "High efficiency germanium immersion gratings," in *Optomechanical Technologies for Astronomy*, edited by Eli Atad-Ettinger Joseph Antebi, Dietrich Lemke, Proceedings of SPIE vol. 6273 (SPIE, Bellingham, WA, 2006) 62733T.
3. E. Hulthen and H. Neuhaus, "Diffraction Gratings in Immersion," *Nature* **173**, pp. 442-443, 1954.
4. N. Ebizuka, M. Iye and T. Sasaki, "Optically anisotropic crystalline gratings for astronomical spectrographs," *Applied Optics* vol. 37, no. 7, pp.1236-1242, March 1 1998.
5. J. T. Rayner, "Evaluation of a solid KRS-5 grism for infrared astronomy," in *Infrared Astronomical Instrumentation*, Albert M. Fowler, Editor, Proceedings of SPIE Vol. 3354, pp.289-294 (1998).
6. J.D. Smith, S.A. Rinehart, J.R.Houck, J.E. Van Cleve, J.C. Wilson, M. Colonno, J. Schoenwald, B. Pirger and C. Blacken, "SCORE 1+: Enhancing a Unique Mid-Infrared Spectrograph," in *Infrared Astronomical Instrumentation*, Albert M. Fowler, Editor, Proceedings of SPIE Vol. 3354, pp.798-809 (1998).
7. P. J. Kuzmenko, "Prospects for machined immersion gratings in the near infrared and visible," in *Optomechanical Technologies for Astronomy*, edited by Eli Atad-Ettinger Joseph Antebi, Dietrich Lemke, Proceedings of SPIE vol. 6273 (SPIE, Bellingham, WA, 2006) 62733S.
8. T.N. Padikal, "Medical physics," Chapter 16 in in *A Physicist's Desk Reference*, 2nd ed., p.229, American Institute of Physics, New York, 1989.

9. O.H. Nestor and C.Y. Huang, "Bismuth germanate: a high-Z gamma ray and charged particle detector," IEEE Transactions on Nuclear Science **NS-22**, pp.68-71, 1975.
10. W.J. Tropf, M.E. Thomas and T.J. Harris, "Properties of Crystals and Glasses," Chapter 33 in *Handbook of Optics vol.2*, 2nd ed., pp. 33.56-33.59, McGraw-Hill, New York, 1995
11. P.A. Williams, A.H. Rose, K.S. Lee, D.C. Conrad, G.W. Day, and P.D. Hale, "Optical, thermo-optic, electro-optic, and photoelastic properties of bismuth germanate (Bi₃Ge₄O₁₂)," Applied Optics **35**, pp.3562-3569, 1996.
12. P. J. Kuzmenko, L. M. Little, P. J. Davis and S. L. Little, "Modeling, Fabrication and Testing of a Diamond-Machined Germanium Immersion Grating," in *IR Space Telescopes and Instruments*, Proceedings of SPIE Vol. 4850, pp.1179-90 (2002)
13. R. Triboulet, "Growth of Zinc Chalcogenides," Chapter 15 in *Crystal Growth Technology* K. Byrappa and T. Ohachi editors (Springer, New York) 2003.
14. E. G. Loewen and E. Popov, *Diffraction Gratings and Applications*, p. 420, Dekker, New York, 1997.
15. Y. Ikeda, N. Kobayashi, P.J. Kuzmenko, S.L. Little, C. Yasui, S. Kondo, A. Minami and K. Motohara, "Diamond-machined ZnSe immersion grating for NIR high-resolution spectroscopy," these proceedings 2008.
16. See www.PhotonicCleaning.com
17. Anantha Murthy R.V.; Ravikumar M.; Choubey A.; Lal K.1; Lyudmila Kharachenko; Shleguel V.; Guerasimov V. "Growth and characterization of large-size bismuth germanate single crystals by low thermal gradient Czochralski method," Journal of Crystal Growth, Volume 197, Number 4, 1 March 1999 , pp. 865-873(9)
18. See website of the Crystal Production Laboratory of the Nikolaev Institute of Inorganic Chemistry, Siberian Branch of the Russian Academy of Sciences <http://eng.che.nsk.su/products/bgo/>

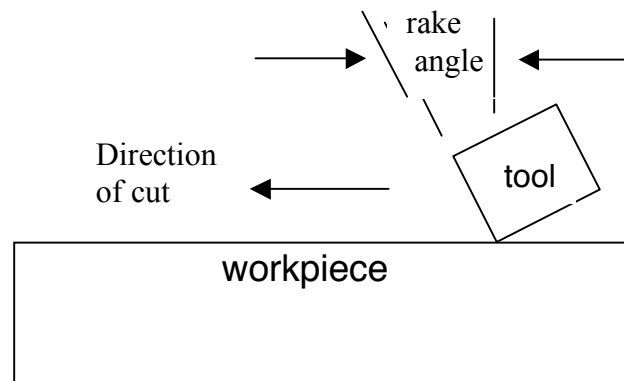


Figure 1 Illustration of a negative rake angle. Negative rake means that the tool is inclined into the workpiece during the cutting process imposing a compressive stress that is essential for ductile cuts in brittle materials.

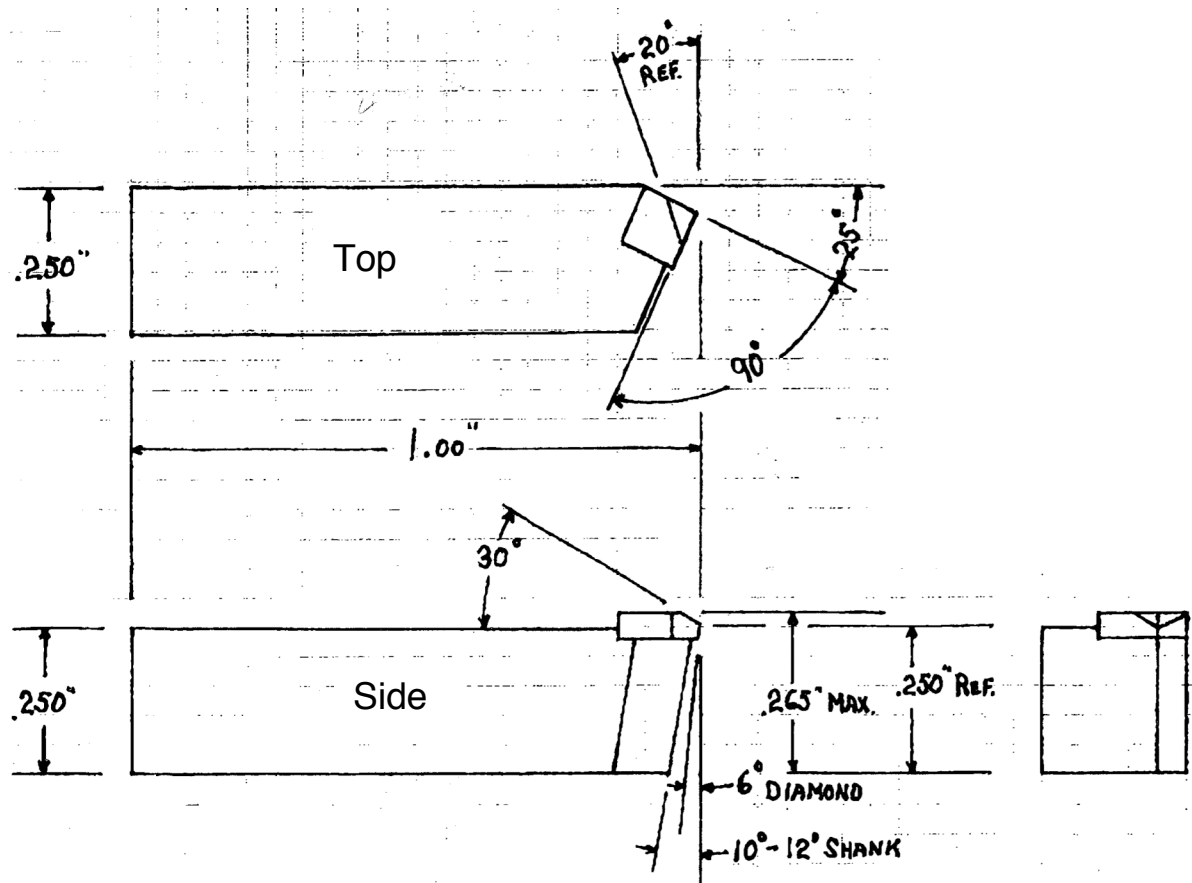


Figure 2 This diamond tool is designed to cut gratings grooves with a blaze angle of 25° (or 65° if one uses the opposite facet). The blaze angle is seen in the top view of the tool. The side view shows the compound angle featuring a double negative rake of 30° .

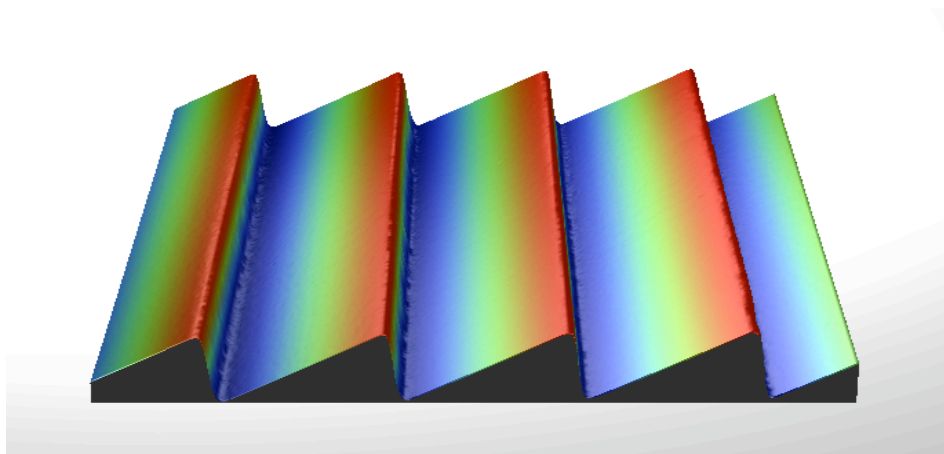


Figure 3 Optical profilometry of $30\ \mu\text{m}$ pitch ZnSe grating flycut at 1000 rpm with a 0.3 inch/minute feed rate shows good groove shape

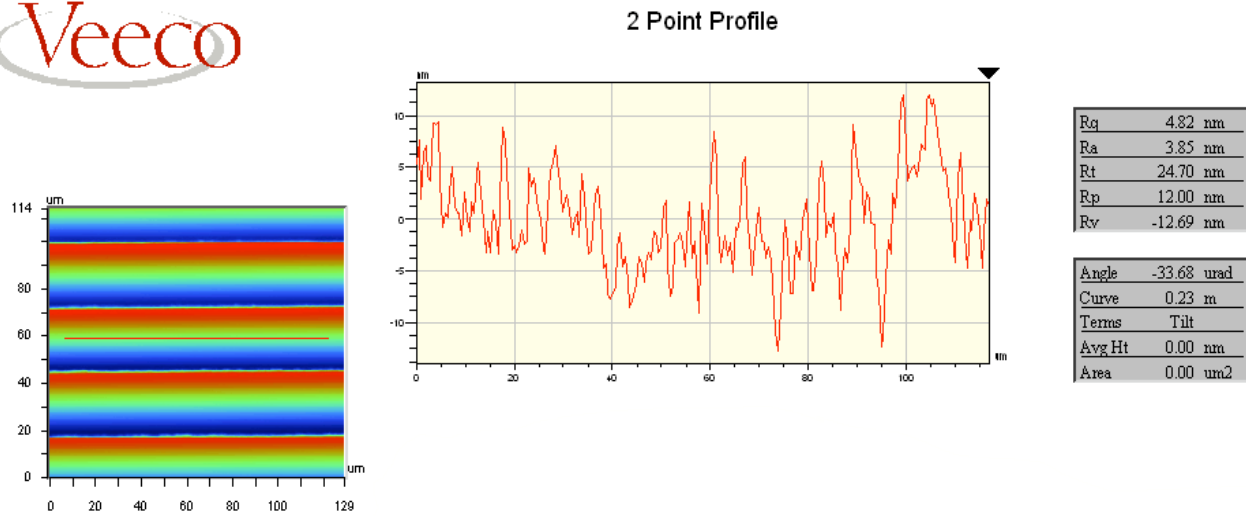


Figure 4 Analysis of linear profile of figure 3 taken parallel to groove shows average surface roughness of < 4 nm

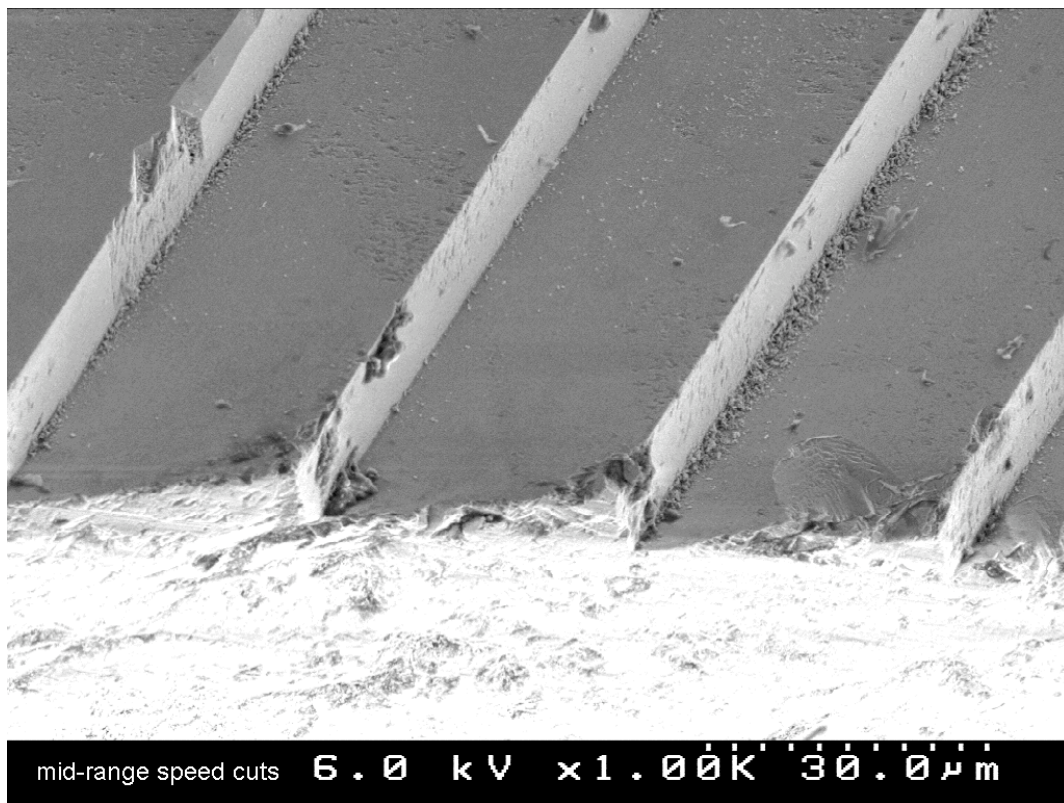


Figure 5 SEM photographs of groove detail of machined ZnSe grating. Some particulates remain on the surface after cleaning.

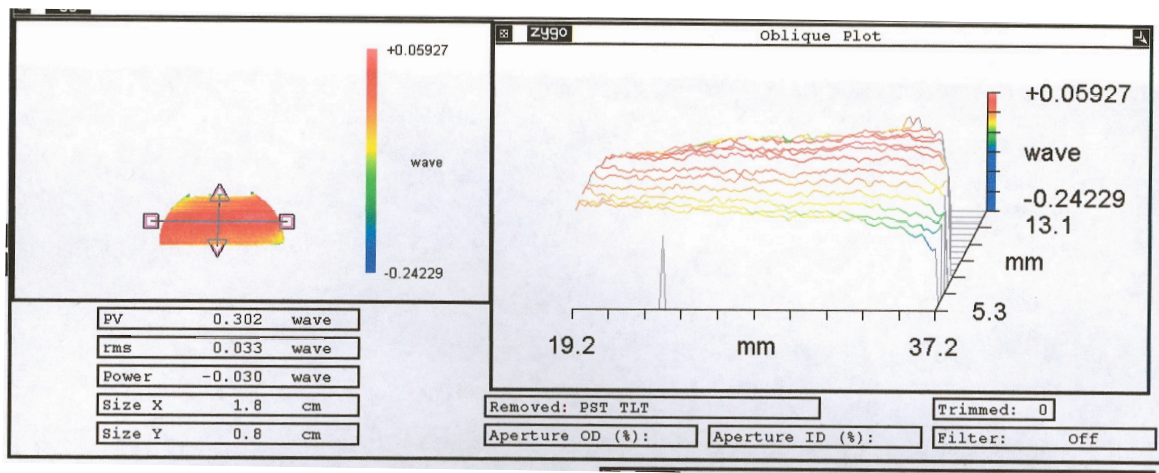


Figure 6 Diffracted wavefront error in 30 μm pitch ZnSe grating is 0.30 wave peak to valley with the largest contribution is near the edges and 0.033 wave rms across the grating. Measurement made at 633 nm wavelength.

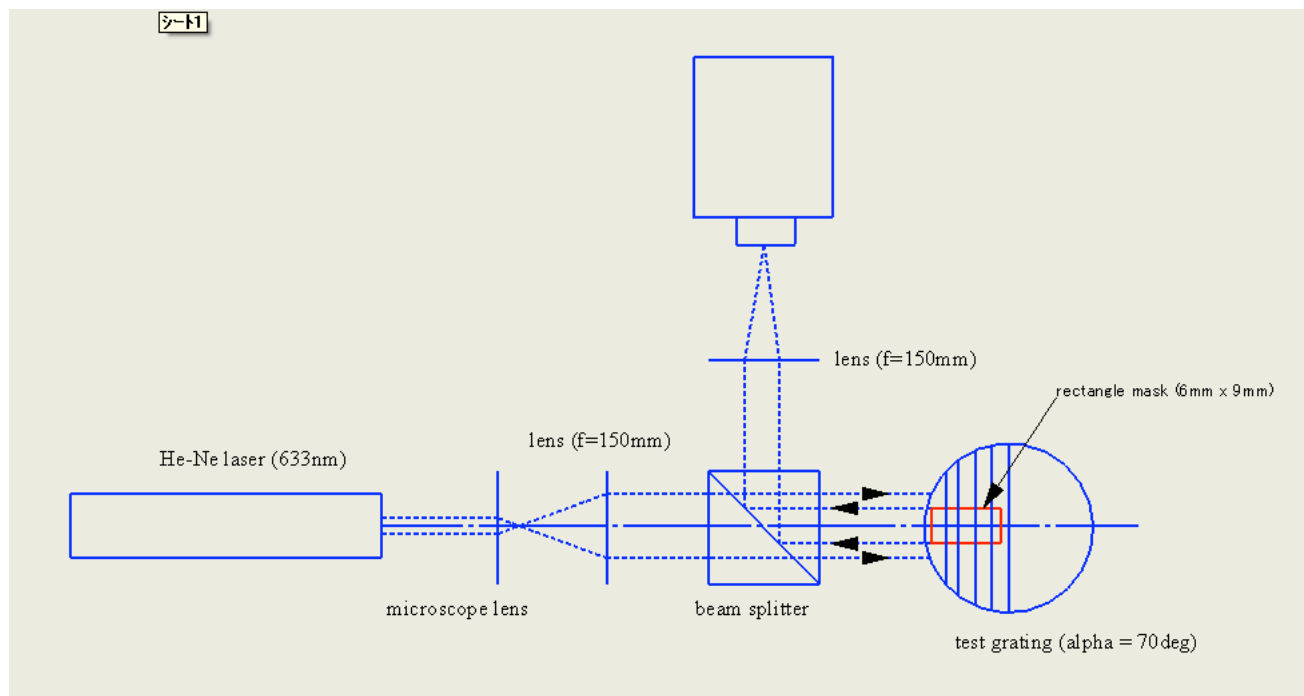


Figure 7 Optical setup for testing ZnSe grating

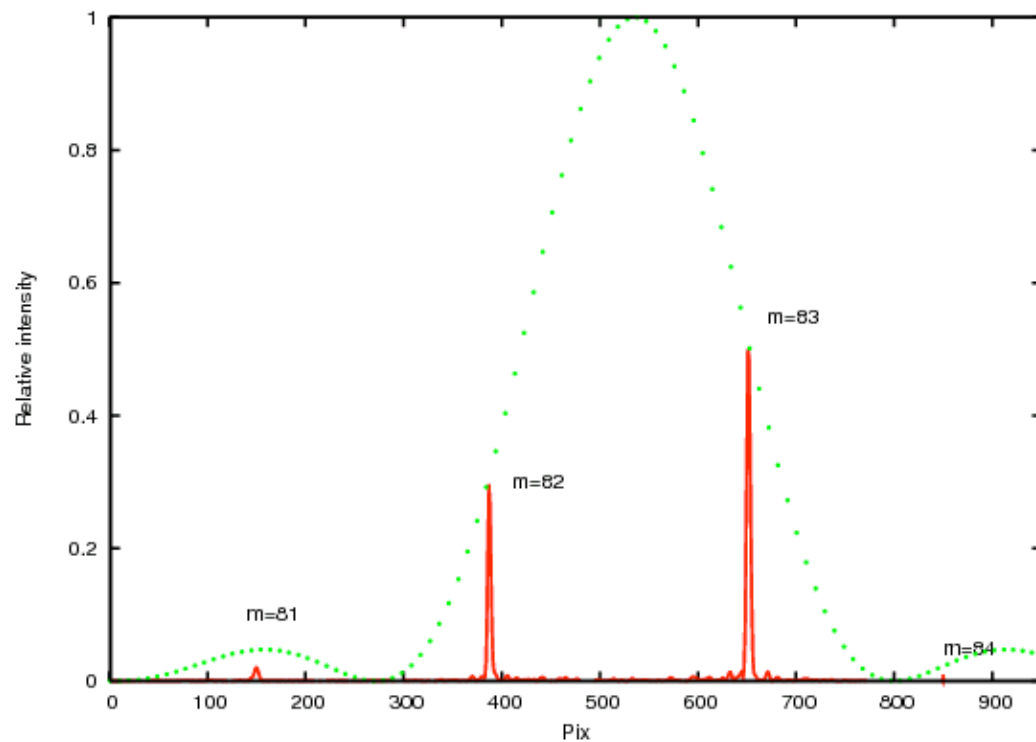


Figure 8 Measured relative intensities of diffracted orders around the blaze angle plotted against the envelope of an ideal blaze function

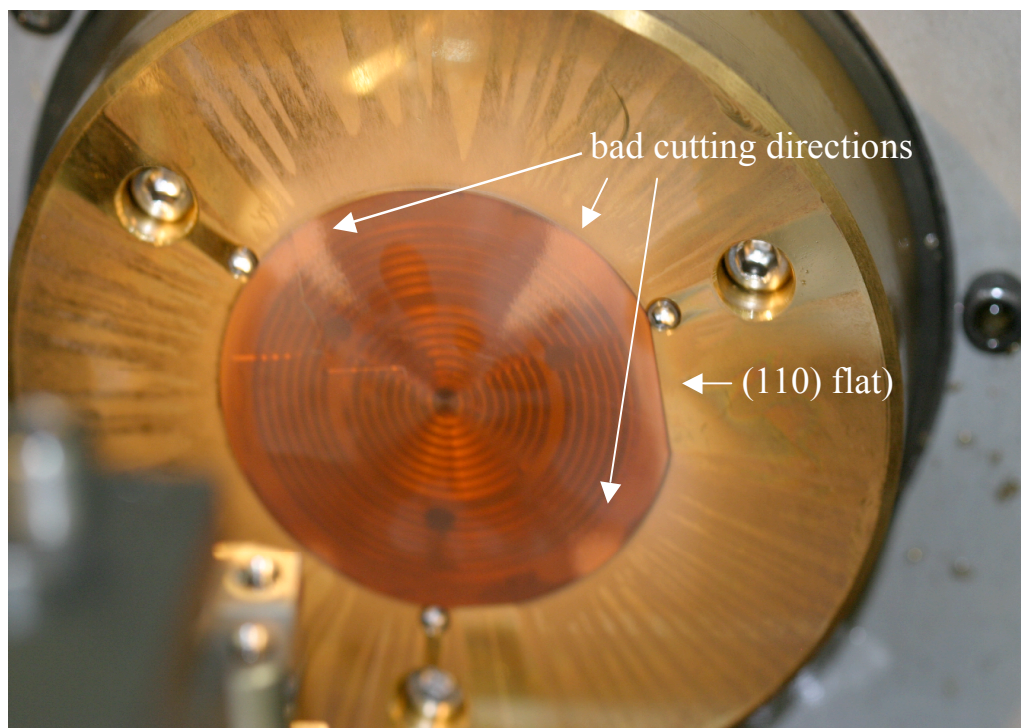


Figure 9 Machined GaP wafer on PERL shows good and bad cutting directions. Tool tip has 762 μ m radius, 40 deg negative rake. Machined at 1000 rpm, 2.5mm/min feed, 0.5 μ m depth of cut, with mineral oil mist. Total of 18 μ m material removed from surface.

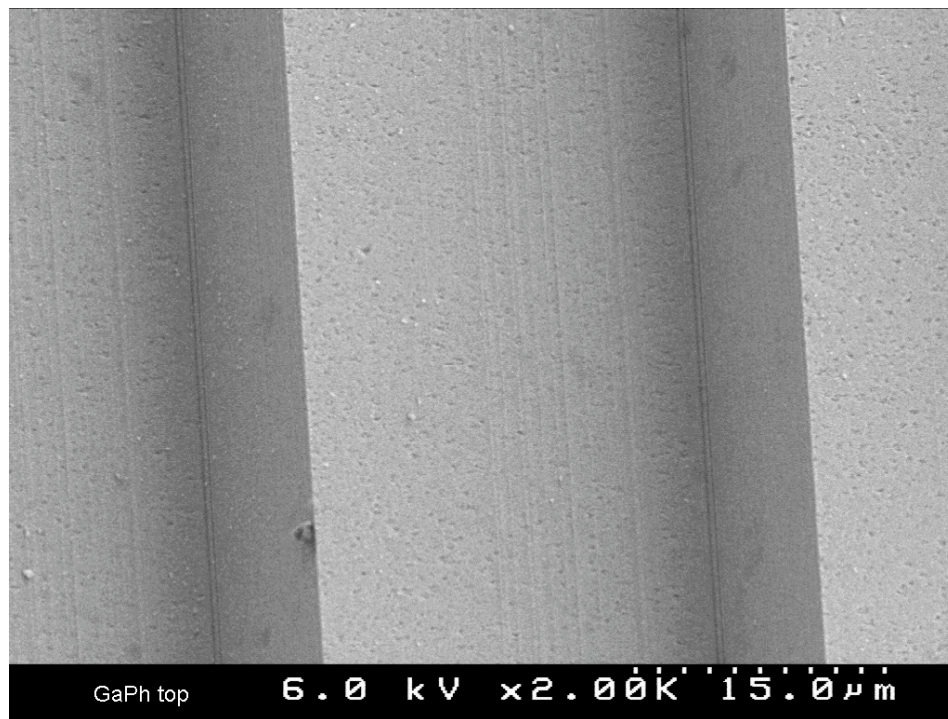


Figure 10 SEM of gallium phosphide grating shows sharp edges to grooves and very few particulates

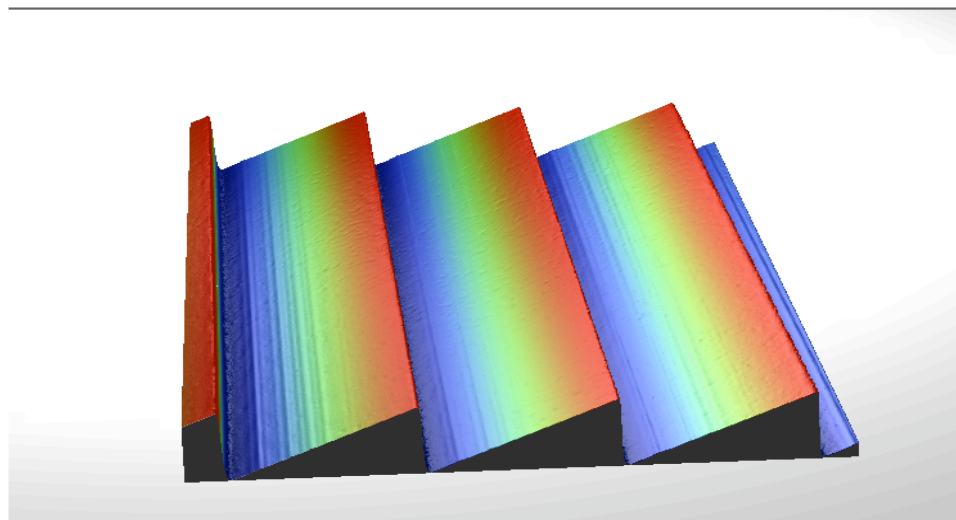


Figure 11 Optical profilometry of GaP rulings indicates good groove quality at a feed rate of 0.4 inch per minute

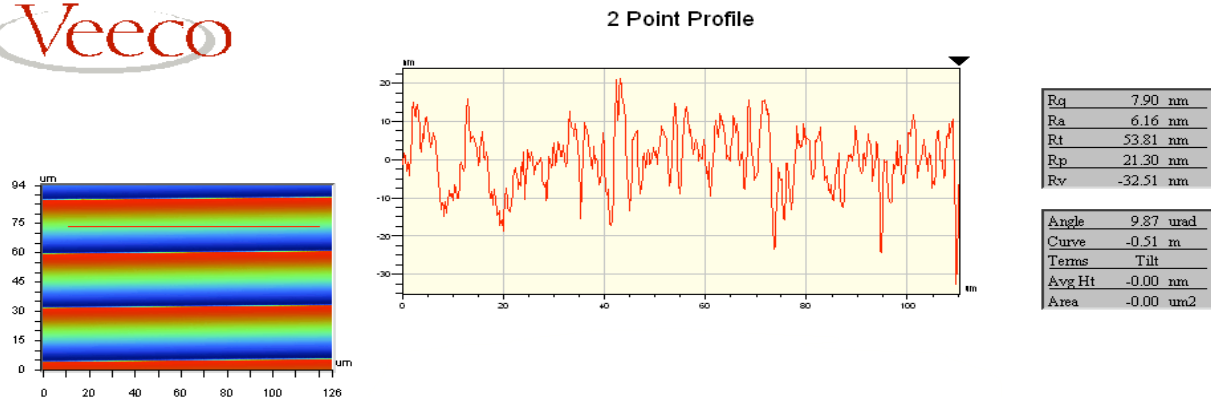


Figure 12 The average roughness parallel to a groove in machined gallium phosphide is about 6 nm.

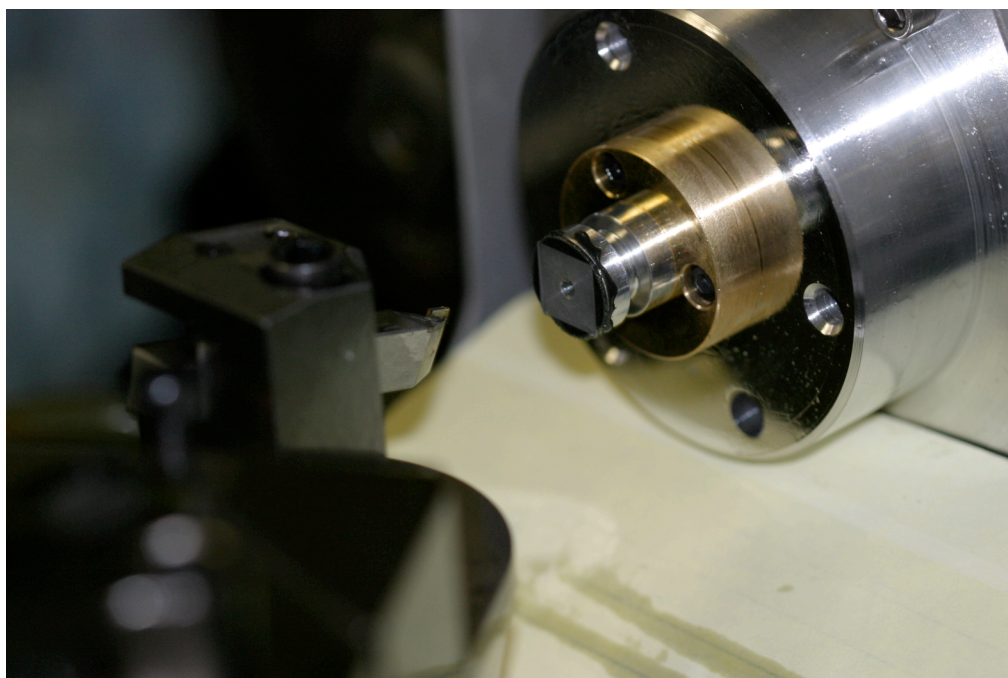


Figure 13 Test setup for machining BGO (square piece glued to spindle)